

# Growth Hormone Synergizes With BMP9 in Osteogenic Differentiation by Activating the JAK/STAT/IGF1 Pathway in Murine Multilineage Cells

Enyi Huang,<sup>1,2</sup> Gaohui Zhu,<sup>2,3</sup> Wei Jiang,<sup>2</sup> Ke Yang,<sup>2,4</sup> Yanhong Gao,<sup>2,5</sup> Qing Luo,<sup>2,3</sup> Jian-Li Gao,<sup>2,6</sup> Stephanie H Kim,<sup>2</sup> Xing Liu,<sup>2,3</sup> Mi Li,<sup>2,3</sup> Qiong Shi,<sup>2,7</sup> Ning Hu,<sup>2,7</sup> Linyuan Wang,<sup>2</sup> Hong Liu,<sup>2,7</sup> Jing Cui,<sup>2,7</sup> Wenwen Zhang,<sup>2,7</sup> Ruidong Li,<sup>2,7</sup> Xiang Chen,<sup>2,8</sup> Yu-Han Kong,<sup>2,7</sup> Jiye Zhang,<sup>2,7</sup> Jinhua Wang,<sup>2,7</sup> Jikun Shen,<sup>2</sup> Yang Bi,<sup>2,3</sup> Joseph Statz,<sup>2</sup> Bai-Cheng He,<sup>2,7</sup> Jinyong Luo,<sup>2,7</sup> Huicong Wang,<sup>1</sup> Feng Xiong,<sup>3</sup> Hue H Luu,<sup>2</sup> Rex C Haydon,<sup>2</sup> Li Yang,<sup>1</sup> and Tong-Chuan He<sup>2,3</sup>

<sup>1</sup>School of Bioengineering, Chongqing University, Chongqing, China

<sup>2</sup>Molecular Oncology Laboratory, Department of Surgery, The University of Chicago Medical Center, Chicago, IL, USA

<sup>3</sup>Stem Cell Biology and Therapy Laboratory of the Key Laboratory for Pediatrics Co-designated by Chinese Ministry of Education and Chongqing Bureau of Education, The Children's Hospital of Chongqing Medical University, Chongqing, China

<sup>4</sup>Department of Cell Biology, Third Military Medical University, Chongqing, China

<sup>5</sup>Department of Geriatrics, Xinhua Hospital of Shanghai Jiatong University, Shanghai, China

<sup>6</sup>Institute of Materia Medica, Zhejiang Chinese Medical University, Hangzhou, China

<sup>7</sup>Key Laboratory of Diagnostic Medicine Designated by the Chinese Ministry of Education, Chongqing Medical University, Chongqing, China

<sup>8</sup>Department of Orthopaedic Surgery, The Affiliated Tangdu Hospital, Fourth Military Medical University, Xi'an, China

## ABSTRACT

Growth hormone (GH) is usually released by somatotrophs in the anterior pituitary in response to the GH-releasing hormone and plays an important role in skeleton development and postnatal growth. However, it is unclear if extrapituitary GH exerts any effect on murine multilineage cells (MMCs). MMCs are multipotent progenitors that give rise to several lineages, including bone, cartilage, and fat. We have identified bone morphogenetic protein 9 (BMP9) as one of the most osteogenic BMPs in MMCs by regulating a distinct set of downstream mediators. In this study, we find that GH is one of the most significantly upregulated genes by BMP9 in mouse MMCs through expression-profiling analysis. We confirm that GH is a direct early target of and upregulated by BMP9 signaling. Exogenous GH synergizes with BMP9 on inducing early and late osteogenic markers in MMCs. Furthermore, BMP9 and GH costimulation leads to a significant expansion of growth plate in cultured limb explants. Although GH alone does not induce de novo bone formation in an ectopic bone formation model, BMP9 and GH costimulated MMCs form more mature bone, which can be inhibited by silencing GH expression. The synergistic osteogenic activity between BMP9 and GH can be significantly blunted by JAK/STAT inhibitors, leading to a decrease in GH-regulated insulin-like growth factor 1 (IGF1) expression in MMCs. Our results strongly suggest that BMP9 may effectively regulate extrapituitary GH expression in MMCs. Thus, it is conceivable that the BMP9-GH-IGF axis may be exploited as an innovative strategy to enhance osteogenesis in regenerative medicine. © 2012 American Society for Bone and Mineral Research.

**KEY WORDS:** BMP9 SIGNALING; EXTRAPITUITARY GROWTH HORMONE; JAK/STAT/IGF1 PATHWAY; MESENCHYMAL STEM CELLS; OSTEOGENIC DIFFERENTIATION

## Introduction

Murine multilineage cells (MMCs) are multipotent progenitors that can undergo self-renewal and differentiate into osteogenic, chondrogenic, adipogenic, and other lineages.<sup>(1-4)</sup>

Although MMCs have been isolated from numerous tissues, one of the major sources in adults is the bone marrow stromal cells. Osteogenesis is a sequential cascade that recapitulates most, if not all, of the cellular events occurring during embryonic skeletal development.<sup>(5)</sup> Bone is one of a few organs that retain the

Received in original form October 26, 2011; revised form March 14, 2012; accepted March 19, 2012. Published online March 29, 2012.

Address correspondence to: Tong-Chuan He, MD, PhD, Molecular Oncology Laboratory, The University of Chicago Medical Center, 5841 South Maryland Avenue, MC 3079, Chicago, IL 60637, USA. E-mail: tche@surgery.bsdu.uchicago.edu or Li Yang, PhD, School of Bioengineering, Chongqing University, Chongqing 400044, China.

E-mail: yangli@cqu.edu.cn

Additional Supporting Information may be found in the online version of this article.

Journal of Bone and Mineral Research, Vol. 27, No. 7, July 2012, pp 1566-1575

DOI: 10.1002/jbmr.1622

© 2012 American Society for Bone and Mineral Research

potential for regeneration into adult life, and is the only tissue that can undergo continual remodeling throughout life. Bone morphogenetic proteins (BMPs) play an important role during development<sup>(4,6–8)</sup> and have been shown to regulate stem cell proliferation and osteogenic differentiation.<sup>(9,10)</sup> BMPs belong to the transforming growth factor  $\beta$  (TGF $\beta$ ) superfamily and consist of at least 14 members in humans.<sup>(4,6–8,11)</sup> Genetic disruptions of BMPs have resulted in various skeletal and extraskeletal abnormalities during development.<sup>(4,11,12)</sup> BMPs initiate their signaling activity by binding to the heterodimeric complex of BMP type I and BMP type II receptors.<sup>(6)</sup> The activated receptor kinases phosphorylate the transcription factors Smads 1, 5, and/or 8, which in turn form a heterodimeric complex with Smad4 and regulate downstream targets in concert with coactivators.<sup>(6)</sup>

By comparing the osteogenic potential of the 14 types of BMPs, we have found that BMP9 is one of the most potent BMPs in inducing osteogenic differentiation of MMCs both in vitro and in vivo by regulating several important downstream targets during BMP9-induced osteoblast differentiation of MMCs.<sup>(8,13–20)</sup> BMP9 (also known as growth differentiation factor 2 [GDF-2]) was first identified in the developing mouse liver,<sup>(21)</sup> and its possible roles include inducing and maintaining the cholinergic phenotype of embryonic basal forebrain cholinergic neurons,<sup>(22)</sup> inhibiting hepatic glucose production and inducing the expression of key enzymes of lipid metabolism,<sup>(23)</sup> and stimulating murine hepcidin 1 expression.<sup>(24)</sup> Nonetheless, BMP9 is one of the least-studied BMPs, and its functional role in the skeletal system remains to be fully understood.

We are intrigued by the fact that growth hormone (GH) is upregulated by BMP9 in MMCs. Among many biological functions, GH plays a critical role in postnatal growth. The regulated secretion of growth hormone in the endocrine system has been well characterized.<sup>(25–31)</sup> In the endocrine system, GH is released by somatotrophs in the anterior pituitary in response to stimulation by GH releasing hormone (GHRH) and is protected from degradation in the bloodstream by serum growth hormone binding protein. However, it has been reported that extra-pituitary GH expression is frequently detected in non-endocrine tissues and/or cells.<sup>(32)</sup> Most tissues and/or cells express GH receptor (GHR),<sup>(25,26,28,30,31)</sup> GH initiates its signaling events by binding to GHR, triggering its tyrosine kinase activity, and activating JAK/STAT and other pathways to fulfill GH's functions in controlling body growth and metabolism.<sup>(25,26,31)</sup> Defects in GH or the GH signaling pathway, such as GH deficiency, GH insensitivity (also known as Laron syndrome), and STAT5b defects, have been shown to be associated with postnatal growth failure.<sup>(25,26,30)</sup> Clinically, recombinant human GH has been used to treat short stature in children, with or without concomitant GH deficiency.<sup>(25,26,29,30)</sup> Nevertheless, it remains to be understood about how GH is regulated, particularly in non-endocrine cells.

In this study, we investigated the role of BMP9-regulated GH expression in MMCs in osteogenic differentiation. Through gene expression profiling analysis, we have found that GH is among one of the most significantly upregulated transcripts by BMP9 in MMCs. We confirm that GH is significantly upregulated by BMP9. Chromatin immunoprecipitation (ChIP) analysis indicates that GH is a direct target of the BMP9/Smad pathway. GH is highly

expressed in the osteoblasts of the growth plate of juvenile long bones. Exogenous GH is shown to synergize with BMP9 on inducing early and late osteogenic markers in MMCs. BMP9 and GH co-stimulation leads to a significant expansion of growth plate of long-bone explants. Although GH alone does not induce de novo bone formation, co-stimulated MMCs with BMP9 and GH form more mature bone in the ectopic bone formation model. The synergistic osteogenic activity between BMP9 and GH is significantly blunted by JAK/STAT inhibitors. Furthermore, GH-regulated IGF1 expression is inhibited by JAK/STAT inhibitors in MMCs. Thus, as a direct target of BMP9 signaling GH synergizes with BMP9 signaling by activating the JAK/STAT/IGF1 pathway and leads to efficient osteogenesis. These findings suggest that a combination of BMP9 and GH may be explored as a novel strategy to enhance osteogenesis in regenerative medicine.

## Materials and Methods

### Cell culture and chemicals

We obtained HEK293 and C3H10T1/2 cells from ATCC (Manassas, VA, USA). Cell lines were maintained in the conditions described.<sup>(13,15,19,33)</sup> JAK Inhibitor I, STAT3 Inhibitor III/WP1066, and STAT5 Inhibitor II/IQDMA were purchased from EMD Chemicals (Gibbstown, NJ, USA). Unless indicated otherwise, all chemicals were purchased from Sigma-Aldrich (St. Louis, MO, USA) or Fisher Scientific (Pittsburgh, PA, USA).

### Isolation of mouse embryo fibroblasts

We isolated mouse embryo fibroblasts (MEFs) from postcoitus day (embryonic day 13.5 [E13.5]) mouse embryos, as described.<sup>(18,19)</sup> Each embryo was dissected into 10 mL sterile PBS, voided of its internal organs, and sheared through an 18-gauge syringe in the presence of 1 mL 0.25% trypsin and 1 mM EDTA. After a 15-minute incubation with gentle shaking at 37°C, DMEM with 10% fetal calf serum (FCS) was added to inactivate trypsin. The cells were plated on 100-mm dishes and incubated for 24 hours at 37°C. Adherent cells were used as MEF cells. Aliquots were kept in a liquid nitrogen tank. All MEFs used in this study were within five passages.

### Recombinant adenoviruses expressing BMP9, GH, and simGH

We generated recombinant adenoviruses using AdEasy technology, as described.<sup>(13,14,34–36)</sup> The coding regions of human BMP9 and GH were PCR-amplified and cloned into an adenoviral shuttle vector and subsequently used to generate recombinant adenoviruses in HEK293 cells. The small interfering RNA (siRNA) target sites against the mouse GH coding region were cloned into the homemade siRNA expression pSES adenoviral shuttle vector<sup>(37)</sup> to generate recombinant adenovirus. The resulting adenoviruses were designated as AdBMP9, AdR-GH, or AdR-simGH. AdBMP9 also expresses green fluorescent protein (GFP), whereas AdR-GH and AdR-simGH express red fluorescent protein (RFP) as a marker for monitoring infection efficiency. Analogous adenovirus expressing only monomeric RFP (AdRFP) or GFP (AdGFP) were used as controls.<sup>(16–19,34,36,38–40)</sup>

## Microarray analysis

We maintained subconfluent C3H10T1/2 cells in Basal Medium Eagle medium containing 0.5% FCS, and infected them with AdBMP9 or AdGFP. At 30 hours after infection, total RNA was isolated, fully characterized, and subjected to hybridizations to Affymetrix mouse gene chips 430A as described.<sup>(18)</sup> The acquisition and initial quantitation of array images were performed using the Affymetrix MAS 5.0 with the default parameters as described.<sup>(15–18,40)</sup> The clustering analysis was carried out using DNA-Chip Analyzer (dChip) software (Cheng Li Lab of Computational Cancer Genomics; <http://www.chengliblab.org>).<sup>(41)</sup> Thresholds for selecting significant genes were set at a relative difference more than twofold, an absolute difference >100 signal intensity units, and a statistical difference at  $p < 0.05$  as described.<sup>(15–18,40)</sup>

## RNA isolation and semiquantitative RT-PCR

We isolated total RNA using TRIZOL Reagents (Invitrogen, Grand Island, NY, USA) and used it to generate cDNA templates by RT reaction with hexamer and Superscript II RT (Invitrogen). The first-strand cDNA products were further diluted 5- to 10-fold and used as PCR templates. Semiquantitative RT-PCR was carried out as described.<sup>(18,19,33,35,40,42–47)</sup> PCR primers (Supplementary Table 1) were designed by using the Primer3 program to amplify the genes of interest (~150–180 bp). A touchdown cycling program was run as follows: 94°C for 2 minutes for 1 cycle; 92°C for 20 seconds, 68°C for 30 seconds, and 72°C for 30 seconds for 12 cycles decreasing 1°C per cycle; and then at 92°C for 20 seconds, 57°C for 30 seconds, and 72°C for 20 seconds for 20 to 25 cycles, depending on the abundance of a given gene. PCR products were resolved on 1.5% agarose gels. All samples were normalized by the expression level of GAPDH.

## Alkaline phosphatase assay

We assessed alkaline phosphatase (ALP) activity by a modified Great Escape SEAP Chemiluminescence assay (BD Clontech, Mountain View, CA, USA) and/or histochemical staining assay (using a mixture of 0.1 mg/mL naphthol AS-MX phosphate and 0.6 mg/mL Fast Blue BB salt), as described.<sup>(13,14,16–19,33,35,40,48,49)</sup> For the chemiluminescence assays, each assay condition was performed in triplicate and the results were repeated in at least three independent experiments. ALP activity was normalized by total cellular protein concentrations among the samples.

## Alizarin Red S staining

We seeded C3H10T1/2 cells and MEFs in 24-well cell culture plates and infected them with AdBMP9, AdRFP, and/or AdR-GH. Infected cells were cultured in the presence of ascorbic acid (50 µg/mL) and β-glycerophosphate (10 mM). At 14 days after infection, mineralized matrix nodules were stained for calcium precipitation by means of Alizarin Red S staining, as described.<sup>(13,14,16–19,33,35,40)</sup> Cells were fixed with 0.05% (vol/vol) glutaraldehyde at room temperature for 10 minutes. After being washed with distilled water, fixed cells were incubated with 0.4% Alizarin Red S (Sigma-Aldrich) for 5 minutes, followed by

extensive washing with distilled water. The staining of calcium mineral deposits was recorded under bright-field microscopy.

## Fetal limb explant culture

We dissected the forelimbs of mouse embryos (E18.5) under sterile conditions and incubated them in DMEM (Invitrogen) containing 0.5% bovine serum albumin (Sigma), 50 µg/mL ascorbic acid (Sigma), 1 mM β-glycerophosphate, and 100 µg/mL penicillin-streptomycin (Mediatech, Manassas, VA, USA) solution at 37°C in humidified air with 5% CO<sub>2</sub> for up to 12 days as described.<sup>(48,49)</sup> The limb explants were directly infected by AdR-GH and/or AdBMP9 24 hours after dissection, 100 mM calcein (Sigma) was added in the medium on the same day, and 50% of the medium was changed every 2 days. Cultured tissues were observed in different time points under a microscope to confirm the survival of cells and the expression of fluorescence markers.

## Immunohistochemical staining

We infected cultured cells with adenoviruses. At the indicated time points, cells were fixed with 10% formalin and washed with PBS. The fixed cells were permeabilized with 1% NP-40 and blocked with 10% goat serum, followed by incubation with an anti-osteocalcin or osteopontin antibody (Santa Cruz Biotechnology, Santa Cruz, CA, USA) for 1 hour. After being washed, cells were incubated with biotin-labeled secondary antibody for 30 minutes, followed by incubating cells with streptavidin-horseradish peroxidase (HRP) conjugate for 20 minutes at room temperature. GH immunohistochemical staining on paraffin-embedded tissues was also carried out with an anti-GH antibody (Santa Cruz Biotechnology). The presence of the expected protein was visualized by diaminobenzidine (DAB) staining and examined under a microscope. Stains with control IgG were used as negative controls.

## Stem cell implantation and micro-computed tomography analysis

We infected C3H10T1/2 cells with AdBMP9/AdRFP, AdBMP9/AdR-GH, or AdBMP9/AdR-simGH. At 16 hours postinfection, cells were harvested and resuspended in PBS for subcutaneous injection ( $5 \times 10^6$ /injection) into the flanks of athymic nude (nu/nu) mice (5 animals per group, 4–6 weeks old, female, Harlan Sprague Dawley). At 4 weeks after implantation, animals were euthanized, and the implantation sites were retrieved for micro-computed tomography (µCT) analysis, histologic evaluation, and other stains.

We imaged all specimens using the µCT component of a GE Triumph (GE Healthcare, Piscataway, NJ, USA) trimodality preclinical imaging system. All image data analysis was performed using Amira 5.3 (Visage Imaging, Inc., San Diego, CA, USA), and 3D volumetric data and bone mean density hit maps were obtained as described.<sup>(48–50)</sup>

## Hematoxylin and eosin, trichrome, and Alcian blue staining

Retrieved tissues were fixed, decalcified in 10% formalin overnight, and embedded in paraffin. Serial sections of the

embedded specimens were stained with hematoxylin and eosin (H&E). Masson trichrome and Alcian blue stains were carried out as described.<sup>(14,17–19,33,35,40,48–50)</sup>

### ChIP analysis

We infected subconfluent C3H10T1/2 cells with AdGFP or AdBMP9. At 30 hours after infection, cells were cross-linked and subjected to ChIP analysis as described.<sup>(18,19,40)</sup> Smad1/5/8 antibody (Santa Cruz Biotechnology) was used to pull down the protein-DNA complexes. The presence of *GH* promoter sequence

was detected by using two pairs of primers corresponding to mouse *GH* promoter region.

### Statistical analysis

All quantitative experiments were performed in triplicate and/or repeated three times. Data were expressed as mean  $\pm$  SD. Statistical significances between vehicle treatment versus drug treatment were determined by one-way analysis of variance and the Student's *t* test. A value of  $p < 0.05$  was considered statistically significant.

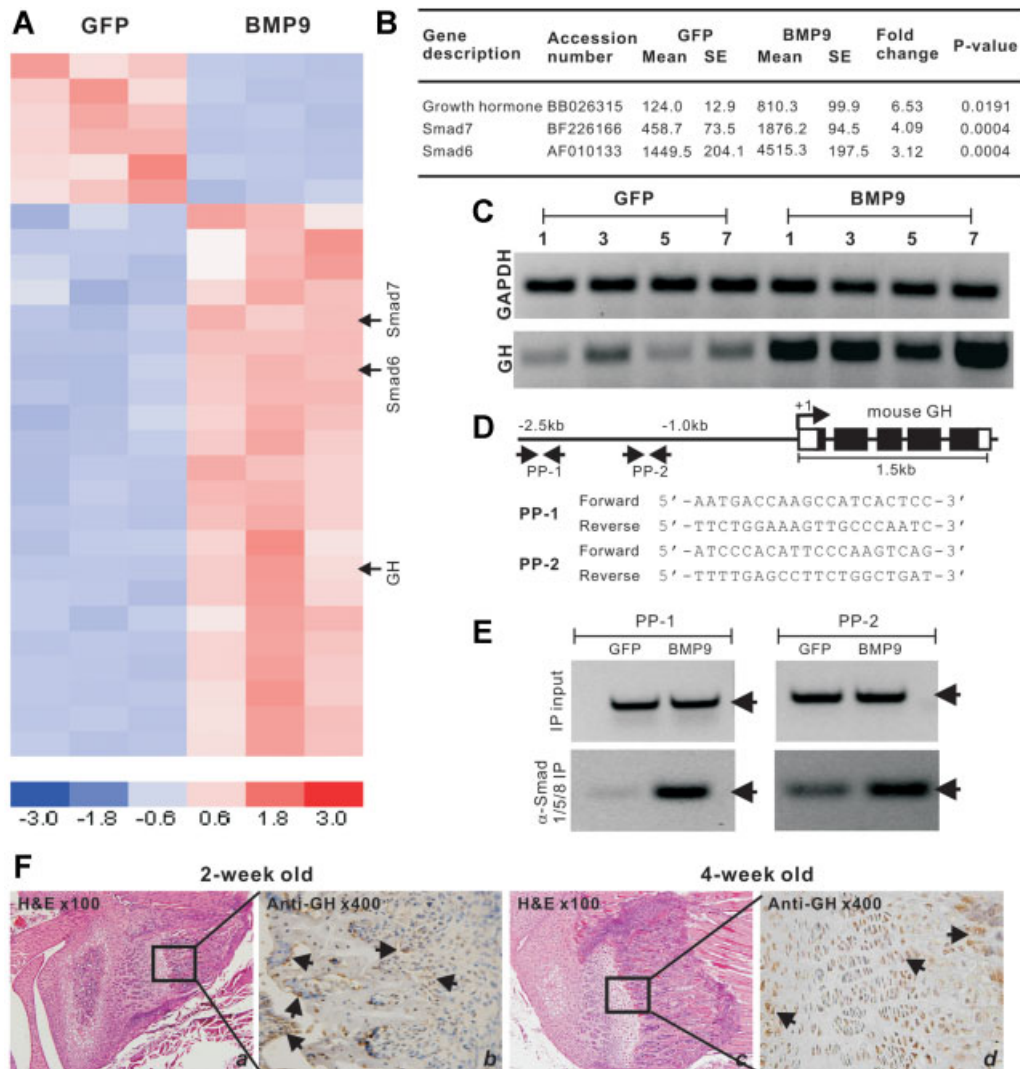


**Fig. 1.** Identification and verification of growth hormone (GH) as an early direct target of BMP9 signaling in MMCs. (A) and (B) dChip clustering analysis of the top 40 most significantly regulated genes by BMP9 in MMCs.<sup>(18)</sup> GH, along with the known BMP9 targets Smad6 and Smad7, was significantly upregulated by BMP9 in MMCs (indicated by arrows). (C) Verification of BMP9-induced GH expression in MMCs. Subconfluent C3H10T1/2 cells were infected with AdBMP9 or AdGFP. Total RNA was collected at the indicated times and subjected to semiquantitative RT-PCR analysis. All samples were normalized for GAPDH expression. Reactions were done in duplicate, and representative results are shown. (D) Schematic depiction of mouse GH promoter region. The approximate locations of the two pairs of primers, PP-1, and PP-2, are indicated. (E) ChIP analysis. Subconfluent C3H10T1/2 cells were infected with AdGFP or AdBMP9. Cells were cross-linked. Genomic DNA was sonicated, following immunoprecipitation with Smad1/5/8 antibody or IgG. The retrieved genomic DNA was subjected to PCR using PP-1 and PP-2. The arrows indicate the locations of the expected products. Control assays demonstrated that a similar amount of input materials was used for immunoprecipitation experiments. The ChIP analysis was performed in three independent experiments, and the representative results are shown. (F) GH expression in developing bone. Long bones (femur) were harvested from 2-week-old and 4-week-old mice, fixed, and paraffin-embedded. The sections were subjected to H&E staining (panels a, c) and immunohistochemical staining with an anti-GH antibody (panels b, d). Isotype IgG was used as a staining control. GH-positive cells are indicated by arrows.

## Results

### GH is upregulated by BMP9 in MMCs

We previously identified that BMP9 is one of the most osteogenic BMPs in MMCs.<sup>(8,13,14,19,20)</sup> Through gene expression profiling analysis, we have found several early targets that are important mediators of BMP9-induced osteogenic signaling.<sup>(15–18,20)</sup> The dChip clustering analysis also revealed that GH was among the top 40 most significantly regulated genes by BMP9 in MMCs (Fig. 1A). GH was upregulated by BMP9 by 6.5-fold, while the known BMP signaling targets Smad6 and Smad7 were only upregulated by 3.1-fold and 4.1-fold, respectively (Fig. 1B). We next sought to verify whether GH expression is regulated by BMP9. When subconfluent C3H10T1/2 cells were infected with AdBMP9 or AdGFP, GH expression was significantly upregulated in BMP9-stimulated MMCs at the tested time points (Fig. 1C). Thus, these results suggest that GH may be an important early target in BMP9-mediated osteogenic signaling.

### GH is a direct target of BMP9-induced Smad signaling

We tested whether GH is a direct target of BMP9-induced Smad signaling pathway using ChIP analysis as described.<sup>(18,19,40)</sup> Mouse GH gene is encoded by five exons that span about 1.5 kb. We analyzed the possible presence of BMP R-Smad binding site(s) in the 2.5-kb GH promoter region using two pairs of PCR primers (Fig. 1D). For ChIP analysis, C3H10T1/2 cells were infected with AdGFP or AdBMP9 and cross-linked. Genomic DNA-protein complexes were immunoprecipitated with anti-Smad1/5/8 antibody. The retrieved genomic DNA was subjected to PCR amplification using the two pairs of primers, PP-1 and PP-2. While the genomic DNA input was comparable among the samples, primer pair PP-1 was shown to amplify the expected fragment in BMP9-stimulated cells, but not in GFP control cells (Fig. 1E). Accordingly, the primer pair PP-2 also amplified the expected product in BMP9-treated cells although the basal level amplification was readily detectable. Nonetheless, these results suggest that GH may be a direct downstream target of BMP9 signaling in MMCs. Consistent with these findings, GH expression was readily detected in the osteoblasts and chondrocytes in the growth plate of developing long bones (Fig. 1F). Furthermore, results of the GH expression in growth plate are supported by other reports about extrapituitary GH expression.<sup>(32)</sup>

### GH potentiates BMP9-induced osteogenic differentiation of MMCs

We next examined the effect of exogenous GH expression on BMP9-induced osteogenic differentiation. To achieve consistent and robust gene expression, we constructed a recombinant adenovirus vectors that express the GH and BMP9 using the AdEasy system.<sup>(13,14,34–36)</sup> To track adenoviral infection efficiency, we incorporated GFP expression cassette in BMP9 viral vector and RFP in GH vector. The generated adenoviruses were shown to effectively transduce MMCs (Fig. 2A). We next transduced MMCs with BMP9, GH alone, or in combination, and determined the effect of GH expression on BMP9-induced early osteogenic marker ALP activity. While exogenous expression of GH alone did

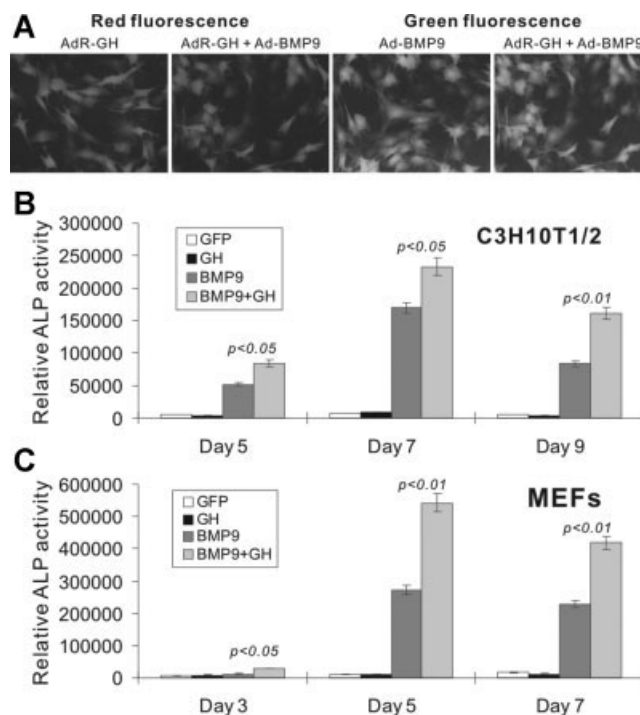


**Fig. 2.** GH potentiates BMP9-induced early osteogenic marker alkaline phosphatase (ALP) in MMCs. (A) Adenoviral vector expressing GH can effectively transduce MMCs. Subconfluent C3H10T1/2 cells were infected with AdBMP9, AdR-GH, or both AdBMP9 and AdR-GH. Red and green fluorescence was examined at 36 hours postinfection. Representative images are shown. (B) and (C) GH potentiates BMP9-induced ALP activity. Subconfluent C3H10T1/2 (B) and MEF (C) cells were infected with AdBMP9, AdR-GH, AdGFP, or AdBMP9 + AdR-GH. Quantitative ALP activity assay was conducted at the indicated time points. Each assay condition was done in triplicate. The results were repeated in at least two independent batches of experiments.

not induce any significant ALP activity, coexpression of BMP9 and GH was shown to synergistically induce ALP activity in C3H10T1/2 cells (Fig. 2B). Similar results were obtained in MEFs (Fig. 2C). These results indicate that GH can potentiate BMP9-induced osteoblast lineage commitment of MMCs.

We further analyzed the effect of GH expression on the late osteogenic markers osteopontin and osteocalcin induced by BMP9 signaling. While GH expression alone failed to induce detectable osteopontin (Fig. 3A panel b) or osteocalcin expression (Fig. 3B panel b), coexpression of BMP9 and GH in MMCs resulted in a stronger expression of osteopontin (Fig. 3A panel d) or osteocalcin (Fig. 3B panel d) than that stimulated by BMP9 alone (Fig. 3A panel c, B panel c). These results reaffirm that GH may act synergistically in BMP9-induced late osteogenic differentiation. Last, we tested the GH's effect on BMP9-induced matrix mineralization. Coexpression of BMP9 and GH resulted in the strongest Alizarin Red S staining of matrix mineralization in C3H10T1/2 cells (Figs. 3C panels d and h), whereas GH alone did not induce any detectable mineralization (Figs. 3C panels b and f). Taking these results together, we have demonstrated that as an important downstream target of BMP9 signaling GH can act synergistically and potentiate BMP9-mediated osteogenic signaling in MMCs.

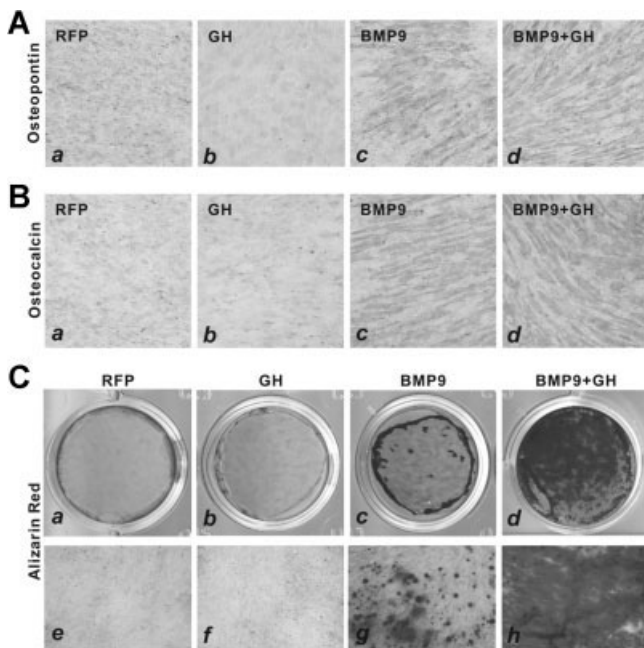


**Fig. 3.** GH potentiates BMP9-induced late osteogenic markers osteopontin and osteocalcin, and matrix mineralization in MMCs. (A, B) Immunohistochemical staining of later osteogenic markers. Subconfluent C3H10T1/2 cells were infected with indicated adenovirus(es). At 10 days postinfection, cells were fixed and stained with anti-osteopontin (A) or anti-osteocalcin (B) antibody. Isotype IgG was used as a staining control. Each assay condition was done in duplicate. Representative results are shown. (C) Alizarin Red S staining of matrix mineralization. Subconfluent C3H10T1/2 cells were infected with indicated adenovirus(es). At 14 days postinfection, cells were fixed and stained with Alizarin Red S solution. The staining results were recorded in lower (panels *a, d*) and higher magnifications (panels *e, h*). The mineralization staining was done in three independent batches of experiments. Representative results are shown.

### GH and BMP9 act synergistically in promoting endochondral ossification in mouse embryo limb explant culture

We sought to analyze the effect of GH on developing bone by using the previously described fetal limb culture assays.<sup>(49)</sup> We infected the isolated E18.5 mouse tibia with BMP9, RFP, and/or GH adenoviruses in culture. New bone formation was indicated by the incorporation of fluorescent dye calcein. The total area of new bone formation was shown to be higher in BMP9 and BMP9 + GH treatment groups, whereas no significant difference existed between RFP and GH treatment groups (Figs. 4A, B). Histologically, BMP9 and GH treatment led to a significantly expansion of the growth plate (Fig. 4C, panel *d* versus panel *a*) although GH or BMP9 alone also showed hypertrophic zone expansion to certain extents (Fig. 4C, panels *b* and *c* versus panel *a*). These results suggest that GH may potentiate BMP9-induced endochondral ossification at growth plate.

### GH accelerates BMP9-induced matrix mineralization during ectopic bone formation

We further carried out stem cell implantation assays to determine the GH effect on BMP9-induced bone formation

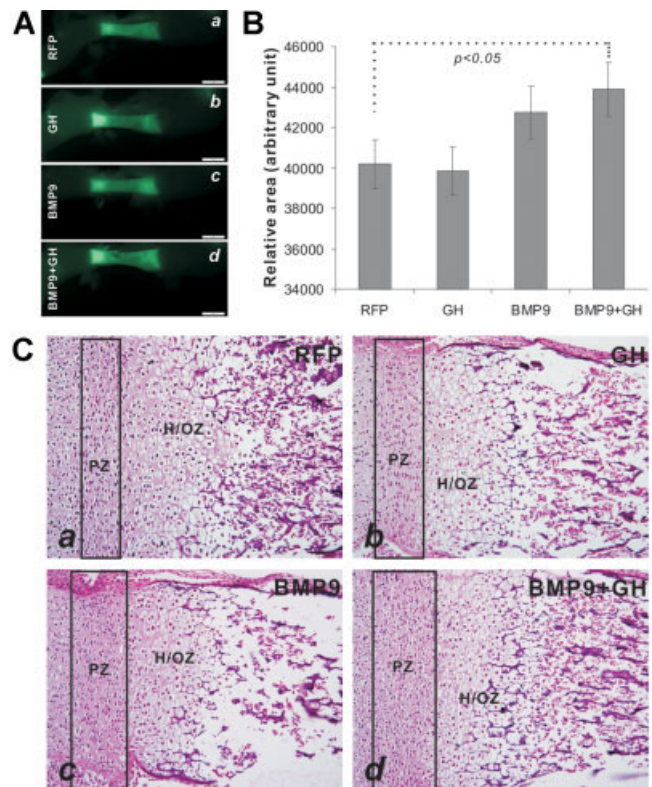


**Fig. 4.** GH and BMP9 act synergistically in promoting endochondral ossification in mouse embryo limb explant culture. (A, B) mouse tibia was isolated from E18.5 embryos and cultured in BSA medium. The cultured explants ( $n = 8$  per assay condition) were infected with BMP9, RFP, and/or GH adenoviruses and continued to culture for 12 days, with medium changed every 2 to 3 days. At day 10, calcein was added to the culture (see Fetal Limb Explant Culture, in Materials and Methods). The tissues were harvested on day 12 and examined under fluorescence microscope (panel *a*), and the fluorescence-positive area for each sample was measured and analyzed (panel *b*). (C) H&E staining. The harvested tissues were fixed, paraffin-embedded, and subjected to H&E staining. The boxed areas indicate the regions with highly proliferative chondrocytes (growth plate), largely corresponding to the P zone. Representative images are shown. H/OZ, hypertrophic/ossification zone; PZ, proliferative zone.

in vivo. When subconfluent C3H10T1/2 cells were co-infected with BMP9, RFP and/or GH and injected into athymic mice subcutaneously, bony masses were found in BMP9 (Fig. 5A panel *a*) and BMP9 + GH (Fig. 5A panel *b*) transduced cell groups at 4 weeks. No masses were formed in the cells transduced with RFP or GH alone. While the gross masses retrieved from BMP9 only and BMP9 + GH groups are not significantly different in size, the 3D iso-surface analysis of the  $\mu$ CT scanning data revealed that the average bone mass in the BMP9 + GH group is larger than that from the BMP9-only group (Fig. 5B). A combination treatment of BMP9 and GH promoted the mineralization of bone masses as demonstrated by  $\mu$ CT analysis of relative bone mean density in Hounsfield unit (Fig. 5C). H&E histologic analysis indicated that MMCs treated with both BMP9 and GH led to significantly more mature and fully mineralized bone matrix than that of the BMP9-alone group (Fig. 5D, panel *b* versus *a*). These results were further confirmed by Masson's Trichrome staining of the retrieved bone masses as more mature

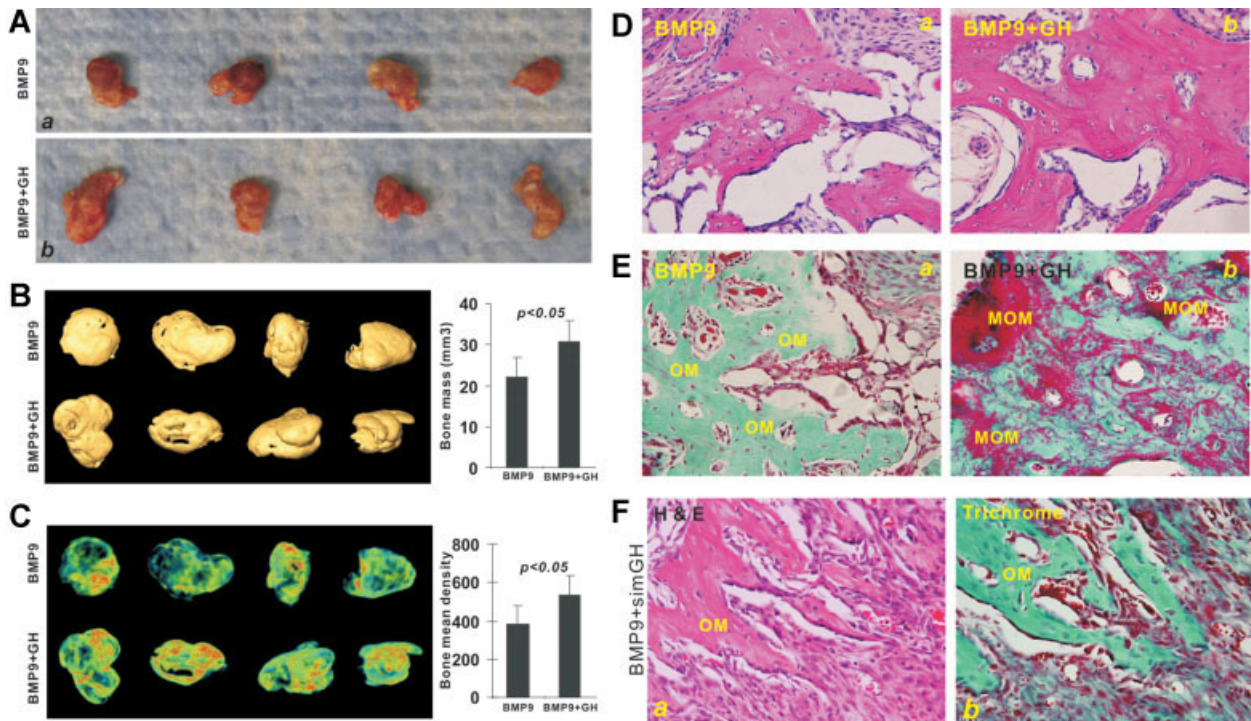


**Fig. 5.** GH accelerates BMP9-induced matrix mineralization in the stem cell implantation assay. Subconfluent C3H10T1/2 cells were co-infected with BMP9, RFP, and/or GH and injected into athymic mice subcutaneously. Bony masses were found in BMP9 and BMP9 + GH transduced cell groups at 4 weeks. No masses of any kind were formed in the cells transduced with RFP or GH alone. (A) Macrographic images of ectopic bone masses formed by BMP9 (panel a) and BMP9 + GH (panel b) MMCs. (B) 3D iso-surface by  $\mu$ CT analysis. The retrieved masses were fixed in formalin and subjected to  $\mu$ CT scanning. The scanning data were analyzed with Amira 5.3 software to obtain 3D iso-surface images and volume rendering (bone mass). (C) Bone mean density measurement. Relative bone density (in Hounsfield units [HU]) was determined using the Amira software. Color red indicates higher HU; green indicates lower HU. (D) H&E staining of the retrieved ectopic bone tissues. (E) Trichrome staining of the retrieved bone masses. (F) Bone masses retrieved from AdR-simGH transduced MMC group were retrieved, fixed, sectioned and stained with H&E (panel a) or Trichrome (panel b). MOM, mineralized osteoid matrix; OM, osteoid matrix.

and mineralized osteoid matrices were found in the specimens treated with both BMP9 and GH (Fig. 5E, panel b versus a). Conversely, MMCs co-infected with AdBMP9 and AdR-simGH formed slightly smaller bone masses and decreased mineralization (Fig. 5F). These results have demonstrated that GH can accelerate BMP9-induced osteoid matrix mineralization.

### GH synergizes with BMP9-induced osteogenic signaling through JAK/STAT/IGF1 pathway, which can be blunted by JAK/STAT inhibitors

We next sought to investigate possible mechanism underlying how GH synergizes with BMP9 action. The GH receptor is a member of the cytokine receptor superfamily and its signaling involves the activation of JAK tyrosine kinases and STAT transcriptional factors.<sup>(26,28,30,31)</sup> We analyzed whether a blockade of JAKs or STATs using their specific inhibitors would blunt the synergy between BMP9 and GH in osteogenic differentiation. When C3H10T1/2 cells were infected with AdBMP9 and AdR-GH or AdRFP, and then treated with JAK Inhibitor I, STAT3 Inhibitor III (or WP1066), or STAT5 Inhibitor II (or IQDMA), BMP9-stimulated ALP activity was significantly inhibited (Fig. 6A). Furthermore, these inhibitors were shown to effectively inhibit the synergistic ALP activity induced by both BMP9 and GH (Fig. 6A). While effective, the tested STAT3 inhibitor is less potent than JAK and

STAT5 inhibitors, suggesting that STAT3 may be not a critical mediator of BMP9-GH signaling relay although further investigation is required. Nevertheless, these data have demonstrated that GH synergizes with BMP9 osteogenic signaling through the activation of JAK/STAT signaling pathway in MMCs.

Classic GH signaling also involves activation of the IGF signaling pathway.<sup>(26,28,30,31)</sup> We further tested whether GH regulates IGF1 expression in MMCs. We infected C3H10T1/2 cells with AdRFP or AdR-GH and found that the expression of IGF1 was upregulated in MMCs upon BMP9 stimulation (Fig. 6B). We sought to determine whether GH-induced IGF1 expression is mediated through the JAK/STAT pathway. Using the JAK/STAT inhibitors, we demonstrated that GH-induced IGF1 expression could be significantly inhibited JAK Inhibitor I, and to a lesser extent, STAT5 Inhibitor II, whereas the STAT3 Inhibitor III was shown to exert little effect under the tested condition (Fig. 6C). Although the exact roles of individual JAK kinases and/or STATs in BMP9-GH signaling relay remain to be thoroughly investigated, our results suggest that GH may play an important role in mediating and synergizing with BMP9 in osteogenesis by activating JAK/STAT/IGF1 signaling pathway in MMCs.

Based on our findings, we propose the following mode of action (Fig. 6D). Upon BMP9 stimulation of MMCs, several important downstream targets including GH are upregulated. GH synergizes with the osteogenic signaling by activating the

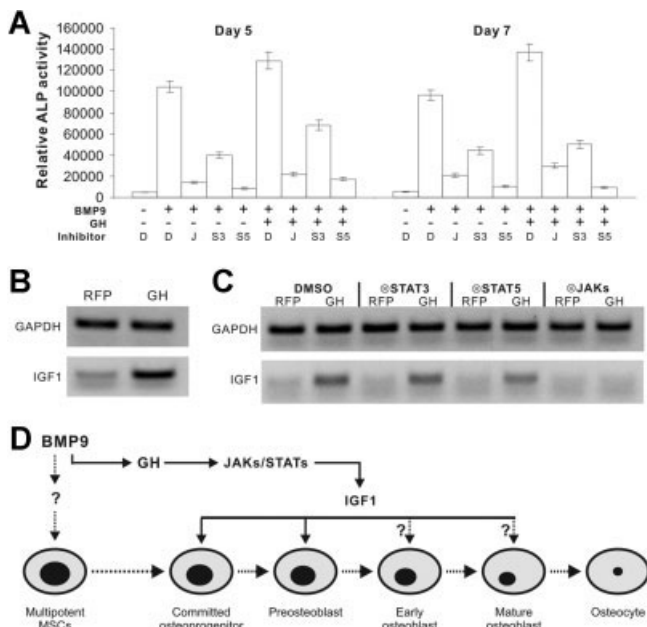


**Fig. 6.** GH functions through JAK/STAT/IGF1 signaling pathway. (A) JAK/STAT inhibitors blunt BMP9-GH synergy. Subconfluent C3H10T1/2 cells were infected with AdBMP9 and AdR-GH or AdRFP. The cells were then treated with JAK Inhibitor I (J, 10  $\mu$ M), STAT3 Inhibitor III/WP1066 (S3, 3  $\mu$ M), STAT5 Inhibitor II/IQDMA (S5, 3  $\mu$ M), or DMSO solvent (D). (B) GH induces IGF1 expression in MMCs. Subconfluent C3H10T1/2 cells were infected with AdRFP or AdR-GH for 72 hours. Total RNA was collected and subjected to RT-PCR analysis using primers specific for mouse IGF1 transcript. GAPDH was used as a normalization standard. (C) GH induces IGF1 through JAK/STAT pathway. C3H10T1/2 cells were infected with AdRFP or AdR-GH, and treated with DMSO control, STAT3 Inhibitor III/WP1066 (3  $\mu$ M), STAT5 Inhibitor II/IQDMA (3  $\mu$ M), or JAK Inhibitor I (10  $\mu$ M) for 72 hours. Total RNA was collected and subjected to RT-PCR analysis using primers specific for mouse IGF1 transcript. GAPDH was used as a normalization standard. (D) A mode of action. Upon BMP9 stimulation of MMCs, important downstream targets including GH are upregulated. GH synergizes with the osteogenic signaling by activating JAK/STAT/IGF1 pathway and leads to efficient osteogenesis.

JAK/STAT/IGF1 axis and leads to efficient osteogenesis (Fig. 6D), although much of the detailed mechanism remains to be fully elucidated.

## Discussion

We have identified BMP9 as one of the most osteogenic BMPs both in vitro and in vivo.<sup>(8,13-20)</sup> As one of the least-studied BMPs, BMP9 may exert its signaling activity by regulating a distinct set of downstream mediators in MMCs. We previously identified several downstream targets in MMCs upon BMP9 stimulation,<sup>(8,15-18,20)</sup> although their exact roles in BMP9-induced osteogenic signaling remain to be elucidated.

Through gene expression profiling analysis, we have found that GH is among one of the most significantly upregulated transcripts by BMP9 in MMCs. We confirm that GH is significantly upregulated by BMP9. CHIP analysis indicates that GH is a direct target of the BMP9/Smad signaling pathway. Histologic evalua-

tion of juvenile long bones reveals that GH is highly expressed in the osteoblasts of the growth plate. Exogenous GH is shown to synergize with BMP9 on inducing early and late osteogenic markers in MMCs. BMP9 and GH co-stimulation leads to a significant expansion of growth plate of long-bone explants. Although GH alone does not induce de novo bone formation, co-stimulated MMCs with BMP9 and GH form more mature bone, which can be diminished by silencing GH expression in MMCs, in the ectopic bone formation model. The synergistic osteogenic activity between BMP9 and GH can be significantly blunted by JAK/STAT inhibitors. Furthermore, GH-regulated IGF1 expression is inhibited by JAK/STAT inhibitors in MMCs. Therefore, as a direct target of BMP9 signaling, GH synergizes with the osteogenic signaling by activating the JAK/STAT/IGF1 pathway and leads to efficient osteogenesis (Fig. 6D) although much of the detailed mechanism remains to be elucidated.

GH is considered as an important hormone for postnatal growth and metabolism.<sup>(25-31)</sup> Defects in GH or the GH signaling pathway, such as GH deficiency, GH insensitivity (aka, Laron syndrome), and STAT5b defects, have been shown to be associated with postnatal growth failure.<sup>(25,26,30)</sup> Accordingly, recombinant human GH has been used to treat short stature in children, with or without concomitant GH deficiency.<sup>(25,26,29,30)</sup> Extr pituitary GH expression is frequently detected in many non-endocrine tissues and/or cells.<sup>(32)</sup> However, it remains to be understood about how GH is regulated particularly in non-endocrine cells. Our findings strongly suggest that GH may be directly regulated by osteogenic BMPs, such as BMP9, in mesenchymal stromal cell-like progenitor cells.

IGF signaling plays an important role in bone and skeletal development and postnatal bone homeostasis.<sup>(51-55)</sup> We previously reported that BMP9 can cross-talk with IGF2 through phosphatidylinositol 3-kinase (PI3K)/protein kinase B (AKT) signaling pathway during osteogenic differentiation of MMCs.<sup>(49)</sup> It is well established that many of growth hormone's physiologic actions are mediated through IGF1.<sup>(27,30,55)</sup> The GH-IGF1 axis is an important part of the pathogenetic mechanisms in the patients with idiopathic short stature (ISS).<sup>(25)</sup> In this study, we have found that BMP9-regulated GH primarily affects IGF1 expression with little effect on IGF2 expression level.

GH transduces its signaling events by binding to GHR, triggering its tyrosine kinase activity, activating JAK/STAT, and regulating IGF1 expression.<sup>(25,26,31,56)</sup> Defects in STAT5b have been shown to be associated with postnatal growth failure.<sup>(25,26,30)</sup> Although JAK2 has been regarded as the classical GHR signaling kinase, strong evidence indicates that activation of the GHR also results in direct activation of src family kinases (SFKs), although the strength of the relative JAK2 and SFK signals is dependent on cell type.<sup>(26)</sup> Our results indicate that the synergistic osteogenic activity between BMP9 and GH can be blunted by JAK/STAT inhibitors, leading to a decrease in GH-regulated IGF1 expression in MMCs.

In summary, we have demonstrated that GH is upregulated by BMP9 and acts synergistically with BMP9 in promoting endochondral osteogenesis in MMCs. The synergistic osteogenic activity between BMP9 and GH can be significantly blunted by JAK/STAT inhibitors, leading to a decrease in GH-regulated IGF1 expression in MMCs. It is conceivable that the BMP-GH-IGF



signaling axis may be exploited as a novel strategy to enhance osteogenesis in regenerative medicine.

## Disclosures

All authors state that they have no conflicts of interest.

## Acknowledgments

We thank Dr. Chad Hanley of the Department of Radiology at The University of Chicago for his assistance and advice on  $\mu$ CT scanning and imaging analysis. This work was supported in part by research grants from the Orthopaedic Research and Education Foundation (RCH and HHL), the National Institutes of Health (RCH, TCH, and HHL), and the Natural Science Foundation of China and Shanghai Education Commission (81101360 and 12YZ053 to YG). EH was a recipient of the Predoctoral Fellowship from the China Scholarship Council.

Authors' roles: Study design: TCH, LY, and EH. Study conduct: EH, GZ, KY, WJ, JLG, JKS, JS. New reagents and analytic tool contribution: YG, XL, ML, HL, JC, WZ, RL, XC, YK, FX, JZ, and JW. Data collection: EH, GZ, KY, and JLG. Data analysis and interpretation: EH, GZ, KY, HW, JLG, TCH, LY, and HHL. Drafting manuscript: All authors. Revising manuscript content: TCH, LY, RCH, HHL, and EH. Approving final version of manuscript: All authors. TCH and LY take responsibility for the integrity of the data analysis.

## References

1. Prockop DJ. Marrow stromal cells as stem cells for nonhematopoietic tissues. *Science*. 1997;276(5309):71–4.
2. Pittenger MF, Mackay AM, Beck SC, Jaiswal RK, Douglas R, Mosca JD, Moorman MA, Simonetti DW, Craig S, Marshak DR. Multilineage potential of adult human mesenchymal stem cells. *Science*. 1999;284(5411):143–7.
3. Aubin JE. Advances in the osteoblast lineage. *Biochem Cell Biol*. 1998;76(6):899–10.
4. Deng ZL, Sharff KA, Tang N, Song WX, Luo J, Luo X, Chen J, Bennett E, Reid R, Manning D, Xue A, Montag AG, Luu HH, Haydon RC, He TC. Regulation of osteogenic differentiation during skeletal development. *Front Biosci*. 2008;13:2001–21.
5. Olsen BR, Reginato AM, Wang W. Bone development. *Annu Rev Cell Dev Biol*. 2000;16:191–220.
6. Shi Y, Massague J. Mechanisms of TGF-beta signaling from cell membrane to the nucleus. *Cell*. 2003;113(6):685–700.
7. Attisano L, Wrana JL. Signal transduction by the TGF-beta superfamily. *Science*. 2002;296(5573):1646–7.
8. Luu HH, Song WX, Luo X, Manning D, Luo J, Deng ZL, Sharff KA, Montag AG, Haydon RC, He TC. Distinct roles of bone morphogenetic proteins in osteogenic differentiation of mesenchymal stem cells. *J Orthop Res*. 2007;25(5):665–77.
9. Varga AC, Wrana JL. The disparate role of BMP in stem cell biology. *Oncogene*. 2005;24(37):5713–21.
10. Zhang J, Li L. BMP signaling and stem cell regulation. *Dev Biol*. 2005;284(1):1–11.
11. Hogan BL. Bone morphogenetic proteins: multifunctional regulators of vertebrate development. *Genes Dev*. 1996;10(13):1580–94.
12. Zhao GQ. Consequences of knocking out BMP signaling in the mouse. *Genesis*. 2003;35(1):43–56.
13. Cheng H, Jiang W, Phillips FM, Haydon RC, Peng Y, Zhou L, Luu HH, An N, Breyer B, Vanichakarn P, Szatkowski JP, Park JY, He TC. Osteogenic activity of the fourteen types of human bone morphogenetic proteins (BMPs). *J Bone Joint Surg Am*. 2003;85-A(8):1544–52.
14. Kang Q, Sun MH, Cheng H, Peng Y, Montag AG, Deyrup AT, Jiang W, Luu HH, Luo J, Szatkowski JP, Vanichakarn P, Park JY, Li Y, Haydon RC, He TC. Characterization of the distinct orthotopic bone-forming activity of 14 BMPs using recombinant adenovirus-mediated gene delivery. *Gene Ther*. 2004;11(17):1312–20.
15. Peng Y, Kang Q, Cheng H, Li X, Sun MH, Jiang W, Luu HH, Park JY, Haydon RC, He TC. Transcriptional characterization of bone morphogenetic proteins (BMPs)-mediated osteogenic signaling. *J Cell Biochem*. 2003;90(6):1149–65.
16. Peng Y, Kang Q, Luo Q, Jiang W, Si W, Liu BA, Luu HH, Park JK, Li X, Luo J, Montag AG, Haydon RC, He TC. Inhibitor of DNA binding/differentiation helix-loop-helix proteins mediate bone morphogenetic protein-induced osteoblast differentiation of mesenchymal stem cells. *J Biol Chem*. 2004;279(31):32941–9.
17. Luo Q, Kang Q, Si W, Jiang W, Park JK, Peng Y, Li X, Luu HH, Luo J, Montag AG, Haydon RC, He TC. Connective tissue growth factor (CTGF) is regulated by Wnt and bone morphogenetic proteins signaling in osteoblast differentiation of mesenchymal stem cells. *J Biol Chem*. 2004;279(53):55958–68.
18. Sharff KA, Song WX, Luo X, Tang N, Luo J, Chen J, Bi Y, He BC, Huang J, Li X, Jiang W, Zhu GH, Su Y, He Y, Shen J, Wang Y, Chen L, Zuo GW, Liu B, Pan X, Reid RR, Luu HH, Haydon RC, He TC. Hey1 basic helix-loop-helix protein plays an important role in mediating BMP9-induced osteogenic differentiation of mesenchymal progenitor cells. *J Biol Chem*. 2009;284(1):649–59.
19. Tang N, Song WX, Luo J, Luo X, Chen J, Sharff KA, Bi Y, He BC, Huang JY, Zhu GH, Su YX, Jiang W, Tang M, He Y, Wang Y, Chen L, Zuo GW, Shen J, Pan X, Reid RR, Luu HH, Haydon RC, He TC. BMP9-induced osteogenic differentiation of mesenchymal progenitors requires functional canonical Wnt/beta-catenin signaling. *J Cell Mol Med*. 2009;13(8B):2448–64.
20. Luther G, Wagner ER, Zhu G, Kang Q, Luo Q, Lamplot J, Bi Y, Luo X, Luo J, Teven C, Shi Q, Kim SH, Gao JL, Huang E, Yang K, Rames R, Liu X, Li M, Hu N, Liu H, Su Y, Chen L, He BC, Zuo GW, Deng ZL, Reid RR, Luu HH, Haydon RC, He TC. BMP-9 induced osteogenic differentiation of mesenchymal stem cells: molecular mechanism and therapeutic potential. *Curr Gene Ther*. 2011;11(3):229–40.
21. Song JJ, Celeste AJ, Kong FM, Jirtle RL, Rosen V, Thies RS. Bone morphogenetic protein-9 binds to liver cells and stimulates proliferation. *Endocrinology*. 1995;136(10):4293–7.
22. Lopez-Coviella I, Berse B, Krauss R, Thies RS, Blusztajn JK. Induction and maintenance of the neuronal cholinergic phenotype in the central nervous system by BMP-9. *Science*. 2000;289(5477):313–6.
23. Chen C, Grzegorzewski KJ, Barash S, Zhao Q, Schneider H, Wang Q, Singh M, Pukac L, Bell AC, Duan R, Coleman T, Duttaroy A, Cheng S, Hirsch J, Zhang L, Lazard Y, Fischer C, Barber MC, Ma ZD, Zhang YQ, Reavey P, Zhong L, Teng B, Sanyal I, Ruben SM, Blondel O, Birse CE. An integrated functional genomics screening program reveals a role for BMP-9 in glucose homeostasis. *Nat Biotechnol*. 2003;21(3):294–301.
24. Truksa J, Peng H, Lee P, Beutler E. Bone morphogenetic proteins 2, 4, and 9 stimulate murine hepcidin 1 expression independently of Hfe, transferrin receptor 2 (Tfr2), and IL-6. *Proc Natl Acad Sci U S A*. 2006;103(27):10289–93.
25. Blair JC, Savage MO. The GH-IGF-I axis in children with idiopathic short stature. *Trends Endocrinol Metab*. 2002;13(8):325–30.
26. Brooks AJ, Waters MJ. The growth hormone receptor: mechanism of activation and clinical implications. *Nat Rev Endocrinol*. 2010;6(9):515–25.
27. Harvey S, Hull KL. Growth hormone. A paracrine growth factor?. *Endocrine*. 1997;7(3):267–79.

28. Hull KL, Harvey S. Growth hormone: a reproductive endocrine-paracrine regulator?. *Rev Reprod.* 2000;5(3):175–82.
29. Park P, Cohen P. Insulin-like growth factor I (IGF-I) measurements in growth hormone (GH) therapy of idiopathic short stature (ISS). *Growth Horm IGF Res.* 2005;15(Suppl A):S13–20.
30. Tanaka H. Growth hormone and bone diseases. *Endocr J.* 1998;45(Suppl):S47–52.
31. Thomas MJ. The molecular basis of growth hormone action. *Growth Horm IGF Res.* 1998;8(1):3–11.
32. Harvey S. Extrapituitary growth hormone. *Endocrine.* 2010;38(3):335–59.
33. Luo X, Chen J, Song WX, Tang N, Luo J, Deng ZL, Sharff KA, He G, Bi Y, He BC, Bennett E, Huang J, Kang Q, Jiang W, Su Y, Zhu GH, Yin H, He Y, Wang Y, Souris JS, Chen L, Zuo GW, Montag AG, Reid RR, Haydon RC, Luu HH, He TC. Osteogenic BMPs promote tumor growth of human osteosarcomas that harbor differentiation defects. *Lab Invest.* 2008;88(12):1264–77.
34. He TC, Zhou S, da Costa LT, Yu J, Kinzler KW, Vogelstein B. A simplified system for generating recombinant adenoviruses. *Proc Natl Acad Sci U S A.* 1998;95(5):2509–14.
35. Kang Q, Song WX, Luo Q, Tang N, Luo J, Luo X, Chen J, Bi Y, He BC, Park JK, Jiang W, Tang Y, Huang J, Su Y, Zhu GH, He Y, Yin H, Hu Z, Wang Y, Chen L, Zuo GW, Pan X, Shen J, Vokes T, Reid RR, Haydon RC, Luu HH, He TC. A comprehensive analysis of the dual roles of BMPs in regulating adipogenic and osteogenic differentiation of mesenchymal progenitor cells. *Stem Cells Dev.* 2009;18(4):545–59.
36. Luo J, Deng ZL, Luo X, Tang N, Song WX, Chen J, Sharff KA, Luu HH, Haydon RC, Kinzler KW, Vogelstein B, He TC. A protocol for rapid generation of recombinant adenoviruses using the AdEasy system. *Nat Protoc.* 2007;2(5):1236–47.
37. Luo Q, Kang Q, Song WX, Luu HH, Luo X, An N, Luo J, Deng ZL, Jiang W, Yin H, Chen J, Sharff KA, Tang N, Bennett E, Haydon RC, He TC. Selection and validation of optimal siRNA target sites for RNAi-mediated gene silencing. *Gene.* 2007;395(1–2):160–9.
38. He TC, Chan TA, Vogelstein B, Kinzler KW. PPARdelta is an APC-regulated target of nonsteroidal anti-inflammatory drugs. *Cell.* 1999;99(3):335–45.
39. He TC, Sparks AB, Rago C, Hermeking H, Zawel L, da Costa LT, Morin PJ, Vogelstein B, Kinzler KW. Identification of c-MYC as a target of the APC pathway. *Science.* 1998;281(5382):1509–12.
40. Si W, Kang Q, Luu HH, Park JK, Luo Q, Song WX, Jiang W, Luo X, Li X, Yin H, Montag AG, Haydon RC, He TC. CCN1/Cyr61 is regulated by the canonical Wnt signal and plays an important role in Wnt3A-induced osteoblast differentiation of mesenchymal stem cells. *Mol Cell Biol.* 2006;26(8):2955–64.
41. Li C, Wong WH. Model-based analysis of oligonucleotide arrays: expression index computation and outlier detection. *Proc Natl Acad Sci U S A.* 2001;98(1):31–6.
42. Bi Y, Huang J, He Y, Zhu GH, Su Y, He BC, Luo J, Wang Y, Kang Q, Luo Q, Chen L, Zuo GW, Jiang W, Liu B, Shi Q, Tang M, Zhang BQ, Weng Y, Huang A, Zhou L, Feng T, Luu HH, Haydon RC, He TC, Tang N. Wnt antagonist SFRP3 inhibits the differentiation of mouse hepatic progenitor cells. *J Cell Biochem.* 2009;108(1):295–303.
43. Zhu GH, Huang J, Bi Y, Su Y, Tang Y, He BC, He Y, Luo J, Wang Y, Chen L, Zuo GW, Jiang W, Luo Q, Shen J, Liu B, Zhang WL, Shi Q, Zhang BQ, Kang Q, Zhu J, Tian J, Luu HH, Haydon RC, Chen Y, He TC. Activation of RXR and RAR signaling promotes myogenic differentiation of myoblastic C2C12 cells. *Differentiation.* 2009;78:195–204.
44. Huang J, Bi Y, Zhu GH, He Y, Su Y, He BC, Wang Y, Kang Q, Chen L, Zuo GW, Luo Q, Shi Q, Zhang BQ, Huang A, Zhou L, Feng T, Luu HH, Haydon RC, He TC, Tang N. Retinoic acid signalling induces the differentiation of mouse fetal liver-derived hepatic progenitor cells. *Liver Int.* 2009;29(10):1569–81.
45. Rastegar F, Gao JL, Shenaq D, Luo Q, Shi Q, Kim SH, Jiang W, Wagner ER, Huang E, Gao Y, Shen J, Yang K, He BC, Chen L, Zuo GW, Luo J, Luo X, Bi Y, Liu X, Li M, Hu N, Wang L, Luther G, Luu HH, Haydon RC, He TC. Lysophosphatidic acid acyltransferase beta (LPAATbeta) promotes the tumor growth of human osteosarcoma. *PLoS One.* 2010;5(12):e14182.
46. He BC, Chen L, Zuo GW, Zhang W, Bi Y, Huang J, Wang Y, Jiang W, Luo Q, Shi Q, Zhang BQ, Liu B, Lei X, Luo J, Luo X, Wagner ER, Kim SH, He CJ, Hu Y, Shen J, Zhou Q, Rastegar F, Deng ZL, Luu HH, He TC, Haydon RC. Synergistic antitumor effect of the activated PPARgamma and retinoid receptors on human osteosarcoma. *Clin Cancer Res.* 2010 Apr 15; 16(8):2235–45.
47. Su Y, Wagner ER, Luo Q, Huang J, Chen L, He BC, Zuo GW, Shi Q, Zhang BQ, Zhu G, Bi Y, Luo J, Luo X, Kim SH, Shen J, Rastegar F, Huang E, Gao Y, Gao JL, Yang K, Wietholt C, Li M, Qin J, Haydon RC, He TC, Luu HH. Insulin-like growth factor binding protein 5 suppresses tumor growth and metastasis of human osteosarcoma. *Oncogene.* 2011 Sep 15; 30(37):3907–17.
48. Zhang W, Deng ZL, Chen L, Zuo GW, Luo Q, Shi Q, Zhang BQ, Wagner ER, Rastegar F, Kim SH, Jiang W, Shen J, Huang E, Gao Y, Gao JL, Zhou JZ, Luo J, Huang J, Luo X, Bi Y, Su Y, Yang K, Liu H, Luu HH, Haydon RC, He TC, He BC. Retinoic acids potentiate BMP9-induced osteogenic differentiation of mesenchymal progenitor cells. *PLoS One.* 2010;5(7):e11917.
49. Chen L, Jiang W, Huang J, He BC, Zuo GW, Zhang W, Luo Q, Shi Q, Zhang BQ, Wagner ER, Luo J, Tang M, Wietholt C, Luo X, Bi Y, Su Y, Liu B, Kim SH, He CJ, Hu Y, Shen J, Rastegar F, Huang E, Gao Y, Gao JL, Zhou JZ, Reid RR, Luu HH, Haydon RC, He TC, Deng ZL. Insulin-like growth factor 2 (IGF-2) potentiates BMP-9-induced osteogenic differentiation and bone formation. *J Bone Miner Res.* 2010;25(11):2447–59.
50. Luo J, Tang M, Huang J, He BC, Gao JL, Chen L, Zuo GW, Zhang W, Luo Q, Shi Q, Zhang BQ, Bi Y, Luo X, Jiang W, Su Y, Shen J, Kim SH, Huang E, Gao Y, Zhou JZ, Yang K, Luu HH, Pan X, Haydon RC, Deng ZL, He TC. TGFbeta/BMP type I receptors ALK1 and ALK2 are essential for BMP9-induced osteogenic signaling in mesenchymal stem cells. *J Biol Chem.* 2010;285(38):29588–98.
51. Linkhart TA, Mohan S, Baylink DJ. Growth factors for bone growth and repair: IGF, TGF beta and BMP. *Bone.* 1996;19(1 Suppl):1S–2S.
52. Dupont J, Holzenberger M. Biology of insulin-like growth factors in development. *Birth Defects Res C Embryo Today.* 2003;69(4):257–71.
53. Rosen CJ. Mouse models for understanding the growth hormone insulin-like growth factor-I axis. *Horm Res.* 2007;68(Suppl 5):2–4.
54. Canalis E. Growth factor control of bone mass. *J Cell Biochem.* 2009;108(4):769–77.
55. Kawai M, Rosen CJ. The IGF-I regulatory system and its impact on skeletal and energy homeostasis. *J Cell Biochem.* 2010;111(1):14–9.
56. Kasukawa Y, Miyakoshi N, Mohan S. The anabolic effects of GH/IGF system on bone. *Curr Pharm Des.* 2004;10(21):2577–92.